ORIGINAL PAPER

Flood vulnerability assessment using the triangular fuzzy number-based analytic hierarchy process and support vector machine model for the Belt and Road region

Yu Duan[1] · Junnan Xiong[1,2] · Weiming Cheng[2,3] · Nan Wang[2,3] · Yi Li[4] · Yufeng He[1] · Jun Liu[1] · Wen He[1] · Gang Yang[1]

Abstract

Flood is one of the most serious natural disasters in the world. Flood losses in the developing countries throughout the Belt and Road region are more than twice the global average. However, to date, the extent of the vulnerability of the Belt and Road region remains poorly understood. Therefore, this study sought to address this knowledge gap. In this study, we presented a vulnerability assessment model based on triangular fuzzy number-based analytic hierarchy process (TFN-AHP) and support vector machine (SVM) model. Firstly, a geospatial database including 11 flood conditioning factors was built. Secondly, the exposure and disaster reduction capability were calculated based on TFN-AHP and SVM, respectively. Finally, the spatial distribution of vulnerability throughout the Belt and Road region was generated. According to the results, the exposure and disaster reduction capability in most areas are extremely low, accounting for 86.45% and 80.53%, respectively. Meanwhile, the vulnerability of 47,105,300 km^2 areas is low or extremely low, accounting for 93% of the Belt and Road region. The high-vulnerable areas (accounting for 3.54%) are primarily concentrated in the southern and eastern parts of China, northern India, most areas of Bangladesh, the Indus Valley in Pakistan, the Nile River Basin in Egypt, and the central region of Indonesia. Obviously, these regions with high vulnerability are characterized by frequent economic activities and dense populations. As suggested of these results, this study provides scientific and technological evidence for the prevention and mitigation of flood disasters in the countries along the Belt and Road region.

Keywords Flood · Vulnerability · Triangular fuzzy number-based analytic hierarchy process · Support vector machine · The Belt and Road region

---

✉ Junnan Xiong
   xiongjn@swpu.edu.cn

Extended author information available on the last page of the article

1 Introduction

Floods rank among the most serious natural disasters in the world. Currently, floods tend to occur more frequently than other disasters (i.e., earthquakes, forest fires, typhoons, heavy snows, and droughts) (Atangana Njock et al. 2020; He et al. 2011). According to recent estimates, the economic losses caused by floods account for 40% of the total losses caused by all natural disasters (Xia et al. 2008). And several studies indicated that frequent flood events had led to an increasing flood risk in the whole world (Hu et al. 2018; Lyu et al. 2019a, b, 2020a; Werren et al. 2016;; Wu et al. 2018). Based on the statistics from the Emergency Disasters Database (EM-DAT, CRED, http://www.emdat.be/), 1,483 floods occurred from 2000 to 2020 in the Belt and Road region, accounting for 44.9% of the total floods around the world. However, most of the countries along the Belt and Road region are developing countries with underdeveloped economies and weak disaster resilience lacking the material reserves and emergency relief capabilities which are needed to respond to disasters (Cui et al. 2020). According to the EM-DAT, the disaster losses in the developing countries along the Belt and Road are more than twice the global average, and the flood-induced mortality is much higher than the global average (Ge et al. 2020). For example, between 2011 and 2013, the Philippines suffered recurrent floods that caused more than 100 fatalities per year, while India and Nepal recorded 6,648 flood fatalities in 2013. Additionally, frequent floods are a major threat to investment and engineering safety and regional development in the Belt and Road region (Ge et al. 2020). More seriously, under future climate change scenarios, the incidence and intensity of flood disasters are likely to increase significantly (Chen et al. 2015;; Fang et al. 2016; Jongman et al. 2012; Ntajal et al. 2017). In this sense, it is of paramount importance and necessity to establish a scientific basis for flood prevention and mitigation in the Belt and Road region.

In the context of the increasing international attention to disaster prevention and mitigation, improving the understanding of vulnerability will contribute to the development of prevention and mitigation measures of floods (Jongman et al. 2015). Theory and previous studies suggest that vulnerability assessment is of great significance to regional and national disaster prevention and mitigation work (Ding et al. 2016; Jongman et al. 2012; Tanoue et al. 2016). Vulnerability studies are currently gaining momentum, and the concept of vulnerability has been widely used in many fields and disciplines, as well as at different spatial levels. Yet, this term varies by discipline and research field (Fraser et al. 2006; Janssen et al. 2006; Liverman and O'Brien 1991; Metzger et al. 2006). For the past decades, the understanding of flood vulnerability has improved due to the use of combined indicators, case studies and analogues, stakeholder-driven processes, and scenario construction methods (Fekete 2012; Malone and Engle 2011). Currently, flood vulnerability is frequently conceptualized as a component that consists of exposure to disturbance or external stress, sensitivity to disturbance, and the capability to adapt or the coping capacity (Adger 2006; Weis et al. 2016; Zhou et al. 2018). In addition, previous studies have shown that flood vulnerability is positively correlated with exposure and negatively correlated with the disaster reduction capability (Rawat et al. 2012). Throughout history, the disaster reduction capability has primarily included susceptibility, resilience, and coping capacity (Bodoque et al. 2016; Ding et al. 2016; Gallopín 2006; Spitalar et al. 2014; Xiong et al. 2019a). Although the concept of the disaster reduction capability varies according to different authors, in this study, it consists of the susceptibility and coping capacity which are both the measure of the physical and social nature of the carrier. Thus, a vulnerability

assessment model that consists of the social exposure, susceptibility, and coping capacity was developed.

The four main types of methods that have been used to assess flood vulnerability include (1) the historical data-based approach (Adikari et al. 2010; Shiet et al. 2011), (2) the scenario simulation method (Li et al. 2010; Shi 2013), (3) the vulnerability curve method (Zong 2013), and (4) the index-based system (Ding et al. 2016; Hoque et al. 2019). The historical data-based approach, which responds to the combined effects of the natural and social vulnerability, is highly practical for vulnerability distillation. However, this method is directly influenced by the level of informativeness of the disaster documentation (Lyu et al. 2020b). The scenario simulation method is a quantitative prediction which is based on the scenario model. Scenario-based vulnerability analysis is typically used to predict flood vulnerability in small areas, but the application of this method is limited by the fact that floods usually occur at the regional scale (Sampson et al. 2012). As for the vulnerability curve method, it primarily focuses on assessing the relationship between the intensity of hazards and the degree to which various hazard-bearing individuals are affected (Shi 2013). However, this method requires field statistics and questionnaires; therefore, it is not suitable for replication and implementation on a large scale. Among the four methods, the index-based system is the most widely applied method in flood vulnerability assessment (Zhang 2014). Notably, the index-based system has the advantages of convenient data acquisition, simple modeling and calculations, and the ability to reflect the regional vulnerability situation at a macroscopic level. Thus, the index-based system was applied in this study. To quantify the indexes more precisely, quantitative research has progressed from the investigation of a single method to that of multiple methods. Generally, these methods include multiple-criteria decision making (MCDM) methods (Lyu et al. 2020b) and machine learning methods (Xiong et al. 2019b). Among the MCDM methods, the triangular fuzzy number-based analytic hierarchy process (TFN-AHP) is one of the most widely used and mature approaches (Lyu et al. 2020b). Additionally, compared with other machine learning methods, the support vector machine (SVM) is a supervised machine learning technique based on statistical learning theory and the principle of structural risk minimization. The SVM not only avoids the effects of human factors, but it also expands the amount of information. Thus, in this study, the TFN-AHP and SVM were used as the quantification methods for the index-based system.

However, the knowledge base regarding large-scale flood risk and vulnerability is quite limited (Jongman et al. 2012). Traditionally, flood vulnerability assessments have been limited to national (de Moel and Aerts 2011; Xiong et al. 2019a) and even regional scales (Bouwer et al. 2010; Lyu et al. 2020b). Based on the physical and social aspects, some scholars have conducted temporal and spatial analyses of the vulnerability of flood disasters in the USA (Cutter and Finch 2008; Spitalar et al. 2014). They concluded that indicator-based vulnerability assessments are the key factors in emergency preparedness, disaster mitigation plannings, immediate responses, and long-term disaster recoveries. At the regional scale, many studies have focused on quantitative methods of vulnerability assessments. This differs from the statistical analyses applied at the national scale. For instance, Ding et al. selected 13 index factors to conduct an assessment of the debris flow vulnerability in the upper reaches of the Min River (Ding et al. 2016). In addition, Lyu et al. applied the AHP and the TFN-AHP in an inundation risk assessment of the metro system in Shenzhen (Lyu et al. 2020b). Their results showed that the TFN-AHP had a higher accuracy than AHP. Obviously, previous studies suggest that the indicator-based system is currently the dominant flood vulnerability evaluation method. However, the application of the methodologies and data used in regional studies has been difficult to apply at larger scales

(Hu et al. 2018; Jongman et al. 2012). In particular, most countries along the Belt and Road region are so underdeveloped that they lack information sharing and international disaster reduction cooperation mechanisms, resulting in many of their fundamental data being inaccurate (Ge et al. 2020). Thus, research regarding the flood vulnerability in the Belt and Road region requires more in-depth investigations, because this region has experienced increasing climate extremes in recent years and is extremely vulnerable to flood disasters currently (Komolafe et al. 2019; Lugeri et al. 2010; Sam et al. 2017).

Given these problems, in this study, a flood vulnerability assessment based on the need for flood disaster prevention and mitigation throughout the Belt and Road region was conducted. The primary objectives of this study are as follows: (1) establish an index system for evaluating the vulnerability of flood disasters throughout the Belt and Road region, including exposure and disaster reduction capability; (2) build a new vulnerability assessment model for large-scale studies based on the TFN-AHP and the SVM to obtain the results of flood vulnerability assessment throughout the Belt and Road region; (3) map and analyze the spatial characteristics of the flood exposure, disaster reduction capability, and vulnerability based on the assessment results.

2 Materials

2.1 Study area

The principle of openness and generosity of the Belt and Road Initiative has led to the absence of precise boundary in the region. Targeting urbanization, we considered 65 developing countries (Liu et al. 2019; Zhou et al. 2020), including China, as the study area (Fig. 1). The countries covered almost all Asian countries except Japan, North Korea and South Korea. In Africa, we only selected Egypt. As for Europe, these countries to the east of Finland, Germany and Austria are all included. Generally, the Belt and Road region
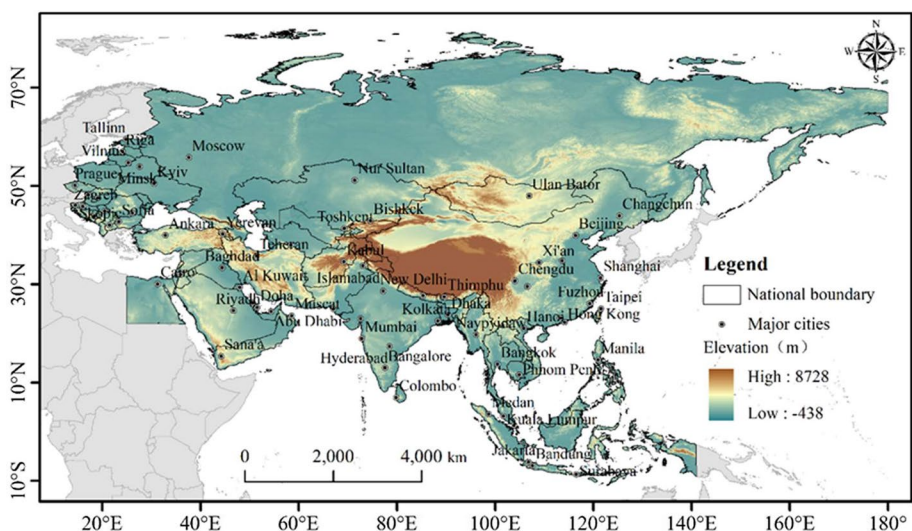
Fig. 1 Location of the Belt and Road region

(approximately 50,640,400 km^2) accounts for 38.5% land area, 30% gross domestic product (GDP), and 62.3% population of this world, respectively (Hafeez et al. 2019). As shown in Fig. 1, this region has an undulating terrain. The highest altitude is greater than 8500 m, while the lowest altitude is less than 0 m. In addition, this region is dominated by eight types of climate, including both monsoons and continental climate characteristics, and the regional distribution of water resources is uneven (Zhou et al. 2020). In terms of precipitation, the average annual total precipitation from 2000 to 2018 increased from 0.92 mm in the northwest to 6,067.71 mm in the southeast in this area. Due to the diverse natural environments, the types of terrains, and the uneven distribution of precipitation, natural disasters, especially droughts and floods, occur frequently in this area. According to the incomplete statistics from the Emergency Disasters Database (EM-DAT, CRED, http://www.emdat.be/), 1561 floods have occurred throughout the Belt and Road Region since the beginning of the twenty-first century, while the number of floods from 1975 to 2000 was only 700 (Hu et al. 2018).

2.2 Datasets and sources

In this study, data related to the flood vulnerability were classified into four aspects: (1) the data related to society and the economy, including population data, land use data, and GDP data. These data were obtained from the World Pop (https://www.worldpop.org/), the National Aeronautics and Space Administration, NASA (https://ladsweb.modaps.eosdis.nasa.gov/), and the Dryad (https://datadryad.org/stash/dataset/doi:10.5061/dryad.dk1j0). Notably, the GDP data on the Dryad came from the Gridded global datasets for Gross Domestic Product and Human Development Index over 1990–2015 (Kummu et al. 2018). (2) The data connected with infrastructure, including data from hospitals, shelters, and road density data, were downloaded from OpenStreetMap (https://www.openstreetmap.org/). (3) The digital elevation model (DEM) data were obtained from the Shuttle Radar Topography Mission (SRTM) data (http://srtm.csi.cgiar.org/srtmdata/). (4) The impervious surface data were collected from the Global Human Settlement Layer, GHSL (https://ghslsys.jrc.ec.europa.eu/). In summary, Table 1 presents the characteristics of the datasets used in this study.

Table 1 Sources and resolutions of the datasets

Factors	Source	Resolution	Type, timeframe
Population	World pop	1×1 km	Raster data, 2015
Land use	National aeronautics and space administration (NASA)	0.5×0.5 km	Vector data, 2015
GDP	Dryad	5 arc-min	Raster data, 2015
Infrastructure	OpenStreetMap	1:50,000	Vector data, 2015
DEM	SRTM data	1×1 km	Raster data, 2010
Impervious surface	Global human settlement layer (GHSL)	30×30 m	Raster data, 2014

2.3 Establishing the assessment index system

2.3.1 Assessment unit

Generally, the assessment results are directly affected by the size and boundary of the assessment units, which are the fundamental elements of vulnerability assessment (Cascini 2008; Li et al. 2012). The assessment units that previous studies have commonly used include regional units, grid units, slope units, topographic units, and uniform condition units (Liu et al. 2017b; Zhou et al. 2014). In this study, the exposure assessment indexes (population density, economic density, building density, and farmland density) were expressed completely as raster maps. In addition, the assessment indexes of the disaster reduction capability (hospital density, shelter density and road density) were expressed as vector maps. The other indexes (impervious surface, the dependent population, female population, and GDP per capita) were expressed in raster format. In order to make a more detailed analysis of all of these indexes, the total study area was divided into 646,191 grid cells with a spatial resolution of $0.1° \times 0.1°$ (12 km*12 km approximately).
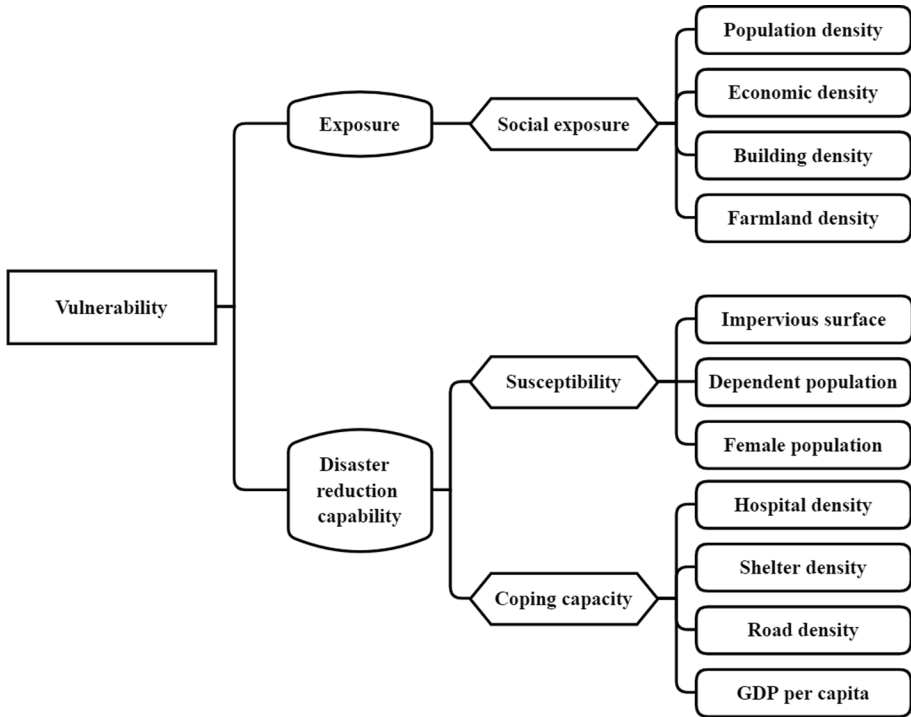
2.3.2 Index system

The establishment of an assessment index system is a key step in building a flood vulnerability assessment. This index system was established after summarizing the results of previous studies which have detailed descriptions of the vulnerability (Ding et al. 2016; Weis et al. 2016; Xiong et al. 2019a). In the numerous previous studies reviewed, vulnerability was most commonly conceptualized as a component consisting of exposure to a disturbance or external stress, sensitivity to a disturbance, and the capability to adapt (Adger 2006; Gallopín 2006). In this study, the disaster reduction capability was regarded as a combination of the susceptibility and coping capacity. Therefore, the flood vulnerability was divided into two portions: the exposure and disaster reduction capability. As shown in Fig. 2, eleven assessment indexes were selected. The exposure indexes consist of population density, economic density, building density, and farmland density. The disaster reduction capability indexes include impervious surface, dependent population, female population, hospital density, shelter density, road density, and GDP per capita.

3 Methodology

3.1 Exposure assessment

3.1.1 Calculation of the exposure indexes

According to previous studies, in areas with higher exposure, the higher the vulnerability, and the greater the losses a flood will cause. Recently, flood vulnerability was divided into two parts: physical vulnerability and social vulnerability (Erena and Worku 2019; Hoque et al. 2019); however, some studies have only analyzed one level, the physical or social level (Rani et al. 2015; Rimba et al. 2017; Susan and Cutter 2003; Zhang and You 2014). In this study, the primary focus was the social level. To some extent, the comprehensive impact of hazards and disasters on the environment was regarded as a threat or danger, while exposed units, such as real estate, farmland, and a human presence, were regarded

Fig. 2 Flood vulnerability assessment index system for the Belt and Road region

as characteristics of the regional socioeconomic system (Huang et al. 2011). Thus, in this study, the population density, economic density, building density, and farmland density were used to calculate the social exposure. In addition, because the exposure factors were measured at different scales, certain reclassifications were necessary to convert the exposure factors into five comparable units or exposure classes: 5 (extremely high exposure), 4 (high exposure), 3 (moderate exposure), 2 (low exposure), and 1 (extremely low exposure) (Mahmoud and Gan 2018). The specific indicators of exposure were defined as follows:

(1) Population density

Population is directly related to flood disasters, and the consequences of flood disasters are also larger in densely populated areas. In this study, the population density represents the population per assessment unit ($D = P_i/S_i$), where D is the population density; P_i is the population of region i; and S_i represents the area of region i.

(2) Economic density

In this study, economic density refers to the GDP per assessment unit ($D = G_i/S_i$), where D is the economic density; G_i is the GDP of region i; and S_i represents the area of region i. Proverbially, the GDP is closely connected to flood disasters. In most cases, regions with higher GDP have stronger disaster adaptation capacity, but the consequences of a flood disaster are also likely to be greater in these regions.

(3) Building density

Building density refers to the building area per assessment unit ($D = B_i/S_i$), where D is the building density; B_i represents the area of buildings in region i; and S_i is the area of region i. Here, the building density was characteristic of using the ratio of the building area to the Belt and Road region, while neglecting the different heights of the buildings.

(4) Farmland density

The farmland density refers to the farmland area per assessment unit ($D = F_i/S_i$), where D is the farmland density, F_i represents the area of farmland in region i; and S_i is the area of region i. In this study, the building density and farmland density factors were both extracted from the land use data, and they indicate the importance of local construction and agricultural activities, respectively.

3.1.2 Triangular fuzzy number-based AHP

In this study, the triangular fuzzy number-based analytic hierarchy process (TFN-AHP) was used to calculate the exposure. In the application of the traditional AHP, since the pair comparison is based on the opinions of the decision makers, the value that represents the relative importance is subjective. The bias that is caused by this subjective importance leads to the uncertainty in the evaluation weight. In comparison, the TFN-AHP is based on the application of a triangular fuzzy number in the traditional AHP, which can reduce the impact of this uncertainty (Lyu et al. 2019a). Instead of the definite number the AHP uses, in the TFN-AHP, a triangular fuzzy number is used to reveal the degrees of importance of the evaluation factors. More detailed, the median value of the triangular fuzzy number denotes the largest probability of the evaluation model, while the minimum and maximum values represent the ambiguity corresponding to the largest probability (Cheng et al. 2020; Lyu et al. 2019a, 2020a; Yang et al. 2013). Generally, the TFN-AHP can assess vulnerability with the largest possibility to improve the accuracy of the results. This is the main reason that the TFN-AHP is selected to calculate exposure in this study. In the application of the TFN-AHP, the triangular fuzzy number is defined as P, and it can be calculated as follows:

$$P = (l, m, \mu)\,(l \leq m \leq \mu) \tag{1}$$

where P is the triangular fuzzy number; m is the most likely value; and l and μ are the minimal and maximum values, respectively. From this we can see that the most probable value for m is jointly determined by the parameters l and μ. The meaning of the triangular fuzzy number and the detailed methods of the parameter calculation have been discussed in previous studies (Lyu et al. 2019a; Zhang and You 2014). In this study, the TFN-AHP was used to confirm the relative significance of each pair of factors by using a 9-point system from 1 (equal importance) to 9 (extreme importance) (Table 2).

In the application of the TFN-AHP, the triangular fuzzy numbers were used in the judgment matrix. Notably, it is of vital importance to construct the triangular fuzzy judgment matrix used in the TFN-AHP. Equation (2) shows a fuzzy judgment matrix of the triangular fuzzy numbers. According to the normalized indexes of the exposure assessment, the corresponding weights of these indexes were calculated using the TFN-AHP, as shown in Table 3.

Table 2 Linguistic variables and the corresponding triangular fuzzy numbers

Linguistic terms	Intensity importance	Triangular fuzzy numbers	Reciprocal triangular fuzzy numbers
Equal importance	1`	(1,1,1)	(1,1,1)
Almost equal importance	1	(1,1,3)	(1/3,1,1)
Intermediate value	2	(1,2,4)	(1/4,1/2,1)
Moderate importance	3	(1,3,5)	(1/5,1/3,1)
Intermediate value	4	(2,4,6)	(1/6,1/4,1/2)
Strong importance	5	(3,5,7)	(1/7,1/5,1/3)
Intermediate value	6	(4,6,8)	(1/8,1/6,1/4)
Very strong importance	7	(5,7,9)	(1/9,1/7,1/5)
Intermediate value	8	(6,8,10)	(1/10,1/8,1/6)
Extreme importance	9	(7,9,11)	(1/11,1/9,1/7)

Table 3 Judgment matrix and normalized weights of the exposure indexes

Exposure	FAD	BUD	ECD	POD	Normalized weights
FAD	(1,1,1)	(0.5,1,1)	(0.2,0.333,1)	(0.143,0.2,0.333)	0.032
BUD	(1,1,2)	(1,1,1)	(0.333,0.5,1)	(0.2,0.25,0.5)	0.110
ECD	(1,3,5)	(1,2,3)	(1,1,1)	(0.25,0.5,1)	0.346
POD	(3,5,7)	(2,4,5)	(1,2,4)	(1,1,1)	0.512

FAD is the farmland density; BUD is the building density; ECD is the economic density; and POD is the population density

$$
\begin{pmatrix}
[1,\ 1,\ 1]\ [l_{12}, m_{12}, \mu_{12}] \cdots [l_{1i}, m_{1i}, \mu_{1i}] \cdots [l_{1n}, m_{1n}, \mu_{1n}] \\
\left[\dfrac{1}{\mu_{12}}, \dfrac{1}{m_{12}}, \dfrac{1}{l_{12}}\right] [1,\ 1,\ 1] \cdots [l_{2i}, m_{2i}, \mu_{2i}] \cdots [l_{2n}, m_{2n}, \mu_{2n}] \\
\cdots \cdots \ \ddots \ \cdots \cdots \cdots \\
\left[\dfrac{1}{\mu_{1i}}, \dfrac{1}{m_{1i}}, \dfrac{1}{l_{1i}}\right] \left[\dfrac{1}{\mu_{2i}}, \dfrac{1}{m_{2i}}, \dfrac{1}{l_{2i}}\right] \cdots [1,\ 1,\ 1] \cdots [l_{in}, m_{in}, \mu_{in}] \\
\cdots \cdots \ \ddots \ \cdots \cdots \cdots \\
\left[\dfrac{1}{\mu_{1n}}, \dfrac{1}{m_{1n}}, \dfrac{1}{l_{1n}}\right] \left[\dfrac{1}{\mu_{2n}}, \dfrac{1}{m_{2n}}, \dfrac{1}{l_{2n}}\right] \cdots \left[\dfrac{1}{\mu_{in}}, \dfrac{1}{m_{in}}, \dfrac{1}{l_{in}}\right] \cdots [1,\ 1,\ 1]
\end{pmatrix}
\tag{2}
$$

3.2 Disaster reduction capability assessment

3.2.1 Calculation of the disaster reduction capability indexes

Previous studies suggest that the higher the disaster reduction capability is, the lower the losses caused by flood disasters will be. In a general sense, susceptibility is the degree or the depth to which the disaster-bearing body is affected by the disaster of the same intensity. Numerous studies have suggested that not all individuals and groups exposed to a hazard are equally susceptible (Hoque et al. 2019; Huang et al. 2011; Liu and Wang 2013). Therefore, data of the impervious surface, dependent populations, and female populations were collected as susceptibility factors. In this study, the coping capability primarily relies on the capability of people, organizations and systems to manage the effects of disasters using the available skills and resources (Rana and Routray 2018). At this level, four coping capability criteria, namely the hospital density, the shelter density, the road density and the GDP per capita, were selected here. The specific disaster reduction capability indicators of flood disasters were selected as follows:

1   Susceptibility
(1)   Impervious surface

Urbanization has an adverse impact on the environment, especially when the urban growth rate and the carrying capacity do not co-evolve, including the management capacity, natural resources, and basic service provisions (Lee et al. 2015). One of the effects of urbanization is an increase in impervious surface, which makes peak discharges intense and rapid.

(2)   Dependent population

Children (0–15 years old) and the elderly (people over 65) were considered to be dependent people, who often need support from other groups when floods are occurring (Li et al. 2012; Sharma et al. 2018). To some extent, children and the elderly often have less access to information and more difficulty in taking personal actions to prepare for floods. In this study, the index of the dependent population was produced using population data.

(3)   Female population

Females are affected by floods in numerous ways due to their limited mobility and difficulty in evacuation during emergency cases (Eric and Thomas 2007; Hoque et al. 2019). Generally speaking, the female population is more vulnerable than the male population.

2   Coping capacity
(1)   Hospital density

The hospitals in this study refer to the large hospitals in modern cities, not those in small regions. Proverbially, the higher the hospital density in a city, the higher the capacity of the people coping with floods and recovering from flood disasters. Moreover, the hospital density refers to the number of hospitals per assessment unit ($D = H_i/S_i$), where D is

the hospital density; H_i is the number of hospitals in region i; and S_i represents the area of region i.

(2) Shelter density

In this study, shelters were defined as the emergency shelters where people can take refuge from flood disasters. The shelter density refers to the number of shelters in an assessment unit ($D = \text{Sh}_i/S_i$), where D is the shelter density; Sh_i is the number of shelters in a region i; and S_i denotes the area of region i.

(3) Road density

Here, roads primarily refer to freeways, provincial highways, and national highways. It is assumed that the higher the road density is, the higher the capacity of the people coping with floods will be. Road density refers to the total length of all types of roads in per assessment unit ($D = R_i/S_i$), where D is the road density; R_i is the total length of all roads in region i; and S_i represents the area of region i.

(4) GDP per capita

The GDP per capita was used to evaluate the economic development level of a grid unit. Throughout history, the GDP per capita is an appropriate indicator of the status, rate, and level of economic development. Generally speaking, the higher the GDP per capita is, the stronger the coping capacity of a region. In this study, the GDP per capita data were calculated by dividing the GDP data by the population data.

3.2.2 Support vector machine

In this study, initially the weights in the indexes of the disaster reduction capability were not clear. In addition, though the TFN-AHP using the fuzzy theory can reduce the subjective influence of an artificial weight determination, it is actually a method of manual weighting which cannot perform completely objectively in the vulnerability assessment. Since TFN-AHP does not completely avoid human intervention, thus, the support vector machine (SVM) was used to calculate the disaster reduction capability. The SVM is a new method developed in recent years that is based on a nonlinear transformation, and it is widely used in flood risk assessment (Xian 2010). Compared with previous models, the SVM method not only avoids the effects of human factors, but it also expands the amount of information (Xiong et al. 2019a). Notably, the SVM is also a supervised learning binary classifier that is based on the structural risk minimization principle (Wan and Lei 2009; Yao et al. 2008), and it can explore the hidden relationships between inputs and outputs (Xu et al. 2012). The mechanism of a flood vulnerability assessment is complex due to the effects of incomplete information and the numerous uncertainties. To reduce the impact of these uncertainties, the SVM model was used to calculate the internal rules based on many complex fuzzy input and output variables. The primary steps of the algorithm are as follows:

(1) Assume a training set of a known sample set is $T = \{x_1, x_2, \ldots, x_n, y\}$, where x_i is the ith input data ($x_i \in R_n$), and y is the output data, $i = 1, 2, \ldots, n$.

(2) Then, these data are classified into two categories, and n-dimensional hyperplanes are used to obtain the maximum interval. This is demonstrated in Eqs. (3) and (4).

$$\frac{1}{2}\|w\|^2 \tag{3}$$

$$\text{Subject to } y_i((w \cdot x_i) + b) \geq 1 \tag{4}$$

where $\|w\|$ represents the norm of the hyperplane normal; b denotes a scale base; and ($\cdot$) is the scalar product operation.

(3) Using the Lagrange multiplier, the definition of the cost function is as follows:

$$L = \frac{1}{2}\|w\|^2 - \sum_{i=1}^{n} \lambda_i(y_i((w \cdot x_i) + b) - 1) \tag{5}$$

where λ_i is the Lagrange multiplier. The solution can be obtained by using the dual minimization of Eq. (6) with w and b (Cherkassky 1997).

(4) For inseparable situations, the constraint conditions can be modified by introducing slack variables, ξ_i (Cherkassky 1997):

$$y_i((w \cdot x_i) + b) \geq 1 - \xi_i \tag{6}$$

Therefore, Eq. (7) becomes:

$$L = \frac{1}{2}\|w\|^2 - \frac{1}{vn}\sum_{i=1}^{n}\xi_i \tag{7}$$

where $v \in (0,1]$, which is introduced to explain the misclassification (Franklin 2005; Xu et al. 2012).

In this study, a kernel function, $K(x_i, x_j)$, was used to make the nonlinear decision boundary clear (Cherkassky 1997). In recent studies, the linear kernel (LN), the polynomial kernel (PL), the sigmoid kernel (SIG), and the radial basis function kernel (RBF) are the kernel types most used for SVM analysis. The RBF was used in this study:

$$K(x_i, x_j) = e^{-\gamma(x_i - x_j)^2}, \gamma > 0 \tag{8}$$

where γ is a parameter of the kernel function.

3.3 Vulnerability assessment

Previous studies have verified that flood vulnerability is positively correlated with the degree of exposure and negatively correlated with the disaster reduction capability (Ding et al. 2016; Rawat et al. 2012). Thus, the vulnerability was calculated by using various data types as proxies for the exposure and disaster reduction capability. Based on previous studies (Ding et al. 2016; Liu and Lei 2003; Xiong et al. 2019a), the vulnerability model was applied using Eq. (9). In this study, using the natural break point method, the results of the exposure, the disaster reduction capability, and the vulnerability were divided into five levels: very low, low, moderate, high, and extremely high (Hoque et al. 2019; Tehrany et al. (2013); (2014).

$$V = E(1 - \sqrt{\text{Re}}) \qquad (9)$$

where V is the vulnerability; E is the exposure; and Re is the disaster reduction capability.

3.4 Assessment procedure

As indicated in Fig. 3, the flowchart consists of three major phases. Firstly, the data that were collected from several websites were preprocessed. The primary step in this phase was normalizing the data and inputting these data into the grids. Subsequently, in the second phase, the data were divided into two aspects: the exposure index and the disaster reduction capability index. After that, the weights of the exposure factors were calculated using the TFN-AHP based on ArcGIS 10.6. As for the calculation of the disaster reduction capability, the factors were input into the SVM model using the R software. In the third phase, the results of the flood vulnerability were mapped and the spatial analysis was conducted.
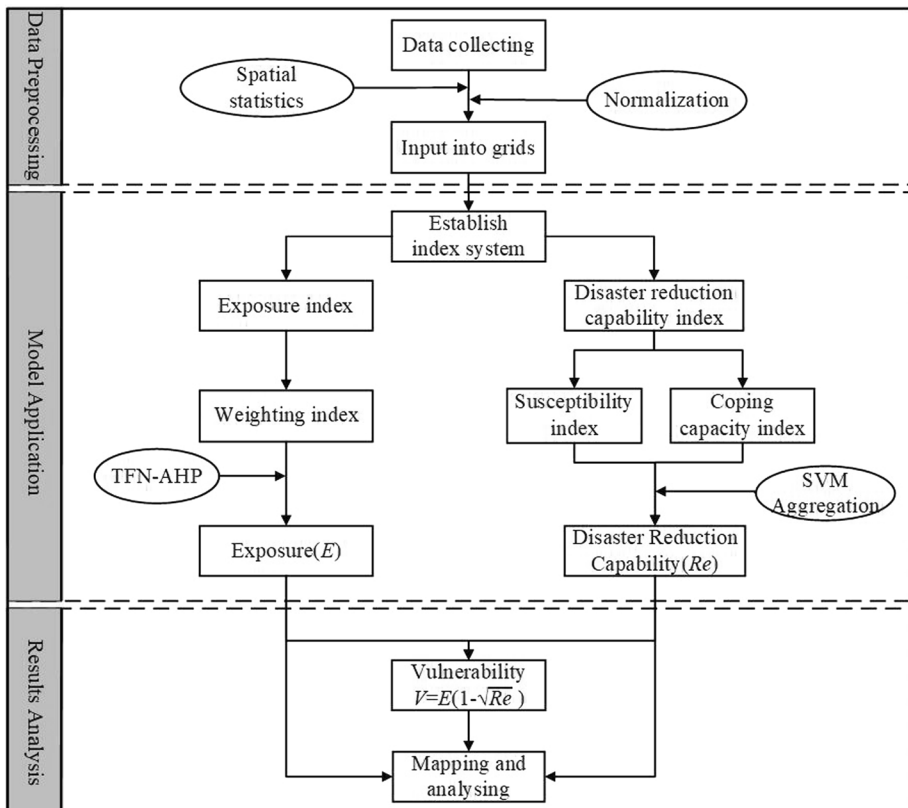
Fig. 3 Flowchart of the flood vulnerability assessment throughout the Belt and Road region

4 Results

4.1 Exposure assessment

In this study, in order to intuitively quantify the results, the exposure was calculated and generated based on ArcGIS 10.6. Then, the results of the exposure were placed into 646,191 grid cells in the ArcGIS 10.6. As illustrated in Table 4, the statistical results of each level of the quantity, area, and proportion in the exposure assessment can be seen. It was discovered that most regions (43,781,500 km^2) have extremely low exposure, accounting for approximately 86% of the total area. The area of the low exposure regions is 3,446,200 km^2, which is larger than the entire area of India. Furthermore, 25,977 grid cells (2,035,700 km^2) have moderate exposure, 13,053 grid cells (1,021,100 km^2) have high exposure, and 4523 grid cells (355,900 km^2) have extremely high exposure. The three levels of exposure only account for approximately 0.70% of the Belt and Road region.

As shown in Fig. 4, a map of the flood exposure throughout the Belt and Road region was produced. It can be seen that the exposure in most areas is low and extremely low. However, in this study, our attention was focused more on those areas with higher exposure, which are likely to suffer more economic and population losses when floods occur. From the perspective of continental scale, the higher exposure areas are primarily located in the eastern and southern parts of Asia, including eastern China, northern India, the Indus Valley in Pakistan, the central region of Indonesia, and most of Bangladesh (Fig. 4). Locally, the areas with extremely high exposure are primarily distributed in the capitals and major cities of the countries in the Belt and Road region, such as Beijing, Shanghai, Chengdu, New Delhi, Bangkok, Jakarta, Moscow, Abu, Riyadh, Kyiv, Baghdad, and Cairo. Obviously, these areas with high exposure are densely populated and economically developed. This is consistent with the larger proportions of the population density and economic density in the exposure indicators.

4.2 Disaster reduction capability assessment

The statistical results of each level of the quantity, area, and proportion of the disaster reduction capability are presented in Table 5. It was found that the disaster reduction capability in most regions is extremely low (407,853,000 km^2) and low (7,869,200 km^2), accounting for 80.53% and 15.54% of the total area, respectively. The areas with moderate disaster reduction capability merely only account for 3.26%. Notably, the areas with high and extremely high disaster reduction capacity both account for less than 1% of the total area. There are only 3,683 grid cells (287,200 km^2) and 648 grid cells (49,300 km^2) having

Table 4 Exposure of floods for the grid cells throughout the Belt and Road region

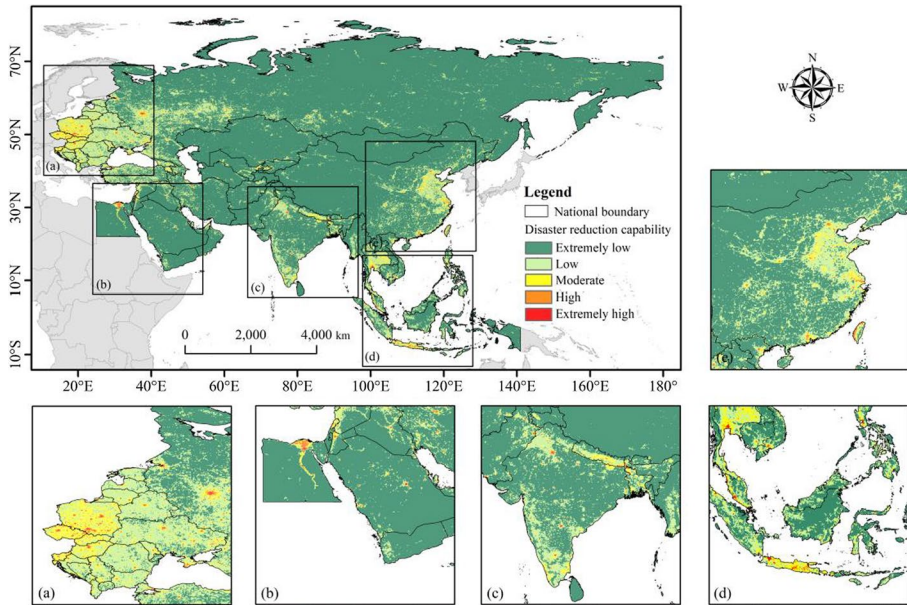| Type	Exposure		
	Count	Area/10000 km^2	Ratio (%)
Extremely low	558,632	4378.15	86.45
Low	44,006	344.62	6.81
Moderate	25,977	203.57	4.02
High	13,053	102.11	2.02
Extremely high	4523	35.59	0.70
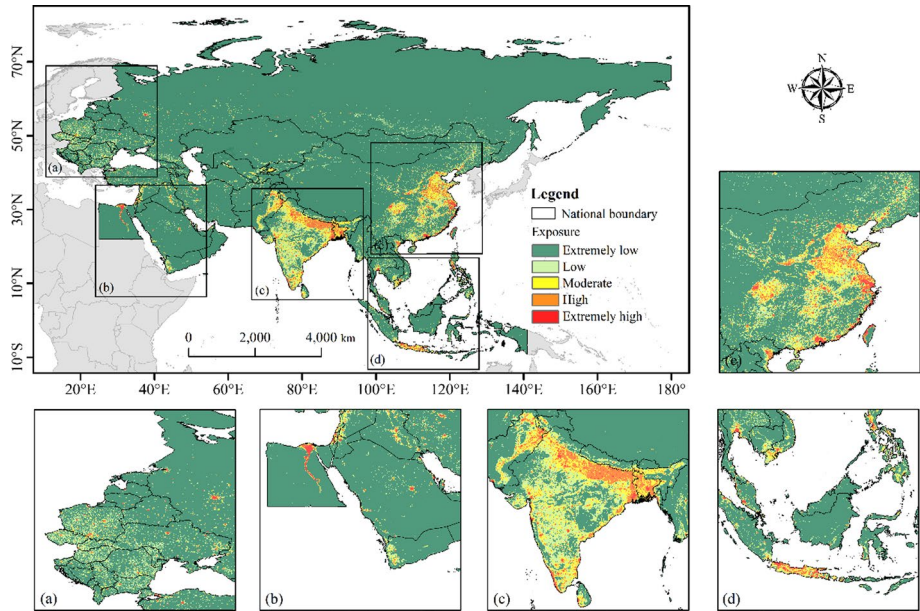
Fig. 4 Spatial distribution of the exposure throughout the Belt and Road region

Table 5 Disaster reduction capability of floods for the grid cells throughout the Belt and Road region

Type	Disaster reduction capability		
	Count	Area/10000 km^2	Ratio (%)
Extremely low	520,377	4078.53	80.53
Low	100,418	786.92	15.54
Moderate	21,065	164.94	3.26
High	3683	28.72	0.57
Extremely high	648	4.93	0.10

high and extremely high disaster reduction capability, accounting for 0.57% and 0.10%, respectively.

As for the spatial distribution patterns, Fig. 5 shows that more than half of the areas have low disaster reduction capability, which is consistent with the above statistical results. The areas with moderate disaster reduction capability are primarily located in the western and eastern parts of the Belt and Road region. Among these areas, only a portion are distributed in eastern China, southern Nepal, the central region of Indonesia and the Cairo region of Egypt, while the vast majority are concentrated in most of the regions of Europe. Notably, few areas have high disaster reduction capability. As shown in Fig. 5, these areas are mainly concentrated in the major cities in the Belt and Road region, such as Beijing, Shanghai, Hong Kong, Taipei, Bangkok, Jakarta, New Delhi, Riyadh, Abu Dhabi, Cairo, Moscow, and several major cities in Europe.

Fig. 5 Spatial distribution of the disaster reduction capability throughout the Belt and Road region

4.3 Vulnerability assessment

According to the assessment results of the exposure and disaster reduction capability, the vulnerability of each grid cell was calculated based on Eq. (9). The statistical results of each grade of the quantity, area, and proportion of the vulnerability are presented in Table 6. As can be seen, vulnerability of most regions (43,817,500 km^2) is extremely low, accounting for 86.53% of the total area. Furthermore, 41,938 grid cells (3,287,800 km^2) have low vulnerability, and 22,229 grid cells (1,744,200 km^2) have moderate vulnerability. In the areas with high and extremely high vulnerability, the disaster distribution density is 1,236,100 km^2 and 554,800 km^2, which account for 2.36 and 1.19% of the total area, respectively.

According to Eq. (9), the vulnerability to floods is positively related to the exposure and negatively related to the disaster reduction capability. Similar to the distribution of the exposure (Fig. 4), most areas have low and extremely low vulnerability, occupying most of the proportion of the Belt and Road region (Fig. 6). In relative terms, the areas with high

Table 6 Vulnerability of floods for the grid cells throughout the Belt and Road region

Type	Vulnerability		
	Count	Area/10000 km^2	Ratio (%)
Extremely low	559,149	4381.75	86.53
Low	41,938	328.78	6.49
Moderate	22,229	174.42	3.44
High	15,767	123.61	2.44
Extremely high	7108	55.48	1.10
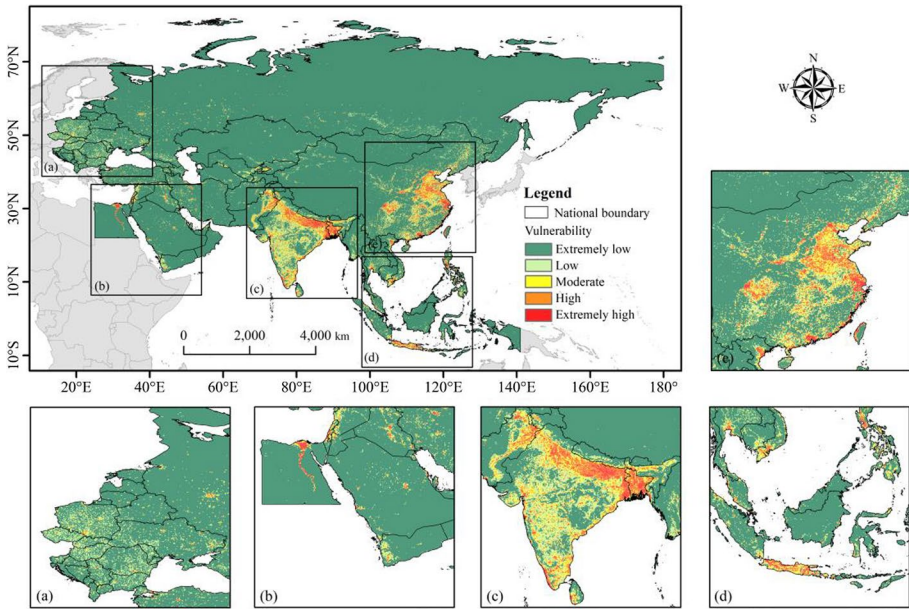
Fig. 6 Spatial distribution of the vulnerability throughout the Belt and Road region

and extremely high vulnerability are primarily distributed in the southern and eastern parts of China, northern India, most of Bangladesh, the Indus Valley in Pakistan, the Nile River Basin in Egypt, the central region of Indonesia, and some major cities in the Belt and Road region. These highly vulnerable areas coincide with the areas characterized by frequent economic activities and dense populations, such as eastern China and northern India, in particular. In contrast to the positive correlation between the exposure and vulnerability, the disaster reduction capability decreases the vulnerability to floods. Thus, those areas with higher disaster reduction capability have lower levels of vulnerability, such as Bangkok of Thailand, Kuala Lumpur of Malaysia, Riyadh in the Kingdom of Saudi Arabia, the Kyiv of Ukraine, and Moscow in Russia.

5 Discussion

5.1 Assessment methodology

In this study, a multi-dimensional analysis of the indexes that were used to calculate the flood vulnerability throughout the Belt and Road region was proposed. In the past decades, many studies have emphasized the importance of quantifying the exposure and disaster reduction capability (Kim and Choi 2011; Li et al. 2010; Xiong et al. 2019a). Thus, the model was extended to a more comprehensive assessment of the flood vulnerability in the Belt and Road region, which included social exposure, susceptibility, and coping capacity. Based on the index-based system, we conducted a flood vulnerability assessment of the Belt and Road region. In addition, we proposed a vulnerability assessment model based on

TFN-AHP and SVM model. To our knowledge, there are currently few studies combining TFN-AHP with SVM model for the flood vulnerability assessment. Compared with previous models, the TFN-based weight is a triangular fuzzy number, not a definite number, which can reduce the impact of these subjectivities on the vulnerability assessment (Lyu et al. 2020b). In addition to the characteristics of the general machine learning methods, the SVM model is a supervised machine learning technique based on statistical learning theory and the principle of structural risk minimization (Bui et al. 2012; Tehrany et al. 2014,2015; Yao et al. 2008).

5.2 The spatial patterns of the exposure, the disaster reduction capability, and the vulnerability to floods.

To our knowledge, there has been no specific attempt to map flood vulnerability by simultaneously considering exposure and disaster reduction capability in the Belt and Road region with high spatial resolution. Our results enhance insight into flood vulnerability drivers, levels of vulnerability to geospatial change, and possible economic and demographic losses. The findings emphasize that countries and regions with dense populations and high economic levels should pay more attention to their disaster prevention and mitigation capabilities, as they tend to have higher vulnerability. Currently, many of the large-scale flood vulnerability studies analyze only at national scale and do not consider refined indicators (Jongman et al. 2015; Tanoue et al. 2016). The findings of this paper provide a reference for a deeper understanding of the vulnerability distribution of the Belt and Road region and the methodology of large-scale vulnerability studies. However, due to the large area of this region, the maximum and minimum values of the data vary greatly, leading to the result that low and extremely low vulnerability occupy most of the area. Future researches could consider these aspects and explore new quantitative and grading methods for large-scale flood vulnerability assessment.

In this study, the results indicate that the vulnerability is positively related to exposure and negatively correlated with the disaster reduction capability (Ding et al. 2016; Xiong et al. 2019a). In fact, there is no vulnerability when the exposure is equal to 0 because "a hazard is not hazardous unless it threatens something; and vulnerability does not exist unless some elements at risk are threatened by something" (Ding et al. 2016). During the assessment procedure, the weights of the assessment indexes have an important influence on the assessment result. Notably, the population density and economic density are key indexes of exposure, while the other indexes are less important (Table 3) (Ding et al. 2016). As shown in Fig. 4, the spatial pattern of the exposure shows that areas with higher population density and economic density have the higher exposure to flood disasters (Ding et al. 2016; Hoque et al. 2019; Tanoue et al. 2016). For instance, in the eastern parts of China, northern India, and the central region of Indonesia, the exposure levels are relatively higher due to the impact of their dense populations and high economic densities (An et al. 2020). In contrast to other areas, numerous capitals and major cities of these countries along the Belt and Road region have higher exposure (i.e., Beijing, Shanghai, Guangzhou, Chengdu, Taipei, Hanoi, Manila, Bangkok, Bandung, New Delhi, Kolkata, Dhaka, Moscow, Cairo, and Abu Dhabi (Fig. 4)). Because capitals are often the political, economic, and cultural centers of their countries. In addition, the exposure of most areas of the Belt and Road region is low and extremely low (Fig. 4), accounting for approximately 93% (Table 4). The reason for this phenomenon is that the maximum and minimum values of these indicators vary too much, although all of the exposure indicators were normalized and reclassified.

With respect to the disaster reduction capability, the findings indicate that the disaster reduction capability of most areas of the Belt and Road region is low, which corresponds to the results of Ge (2020) and Cui (2020), who demonstrated the weak disaster prevention and mitigation capabilities throughout the Belt and Road region. As shown in Fig. 5, most areas of the Belt and Road region have extremely low (40,785,300 km^2) and low (7,869,200 km^2) disaster reduction capability, accounting for 80.53% and 15.54% of the total area, respectively (Table 5). Notably, most of the countries in this region have underdeveloped economies, low levels of education, and high population densities, leading to the weak disaster prevention and resilience capabilities (Cui et al. 2020). In contrast, the more developed cities and regions have higher disaster reduction capability (i.e., Beijing, Shanghai, Chengdu, Guangzhou, Taipei, Hanoi, Bangkok, Kuala Lumpur, Dhaka, New Delhi, Moscow and Abu Dhabi). Regionally, the areas with higher disaster reduction capability are primarily distributed in the European countries, while a small amount is located in eastern China, the central region of Indonesia, the Cairo region of Egypt, and several cities in western Russia (Fig. 5). The people in these areas can respond quickly to flood disasters and have the strong resistance to disaster losses (Jongman et al. 2012; Okazawa et al. 2011). In addition, the spatial patterns of the disaster reduction capability reveal that the areas with high hospital densities, high shelter densities, high road densities and high GDP per capita have a lower incidence of flood disasters (Hoque et al. 2019), especially in the European countries (Fig. 5).

The results presented here support some of the important findings of previous studies. Similar to the observations reported in several studies (Fang et al. 2015; Liu et al. 2017a; Liu et al. 2018), the resulting vulnerability throughout the Belt and Road region (Fig. 6) indicates that the distribution characteristics of the vulnerability are similar to that of the population density and GDP. In general, the spatial distribution of the vulnerability (Fig. 6) is similar to that of the exposure (Fig. 4), which is in agreement with Eq. (9). Compared to earlier models which calculate vulnerability through the direct addition of the exposure, susceptibility, and coping capacity, the information used in the approach proposed in this study is expanded (Ding et al. 2016). It can be seen from Fig. 6 that the vulnerability of most regions (43,817,500 km^2) is extremely low, accounting for 86.53% of the total area. Regionally, those areas with extremely high vulnerability are primarily distributed in eastern China, northern India, the Indus Valley in Pakistan, and most of Bangladesh, which are densely populated and economically concentrated. When these areas suffer from floods, the flood-induced mortality and economic losses in these areas will be more severe than in other areas. Additionally, the level of vulnerability in many major cities (Fig. 6) is lower than that of the exposure (Fig. 4) due to their higher disaster reduction capabilities (Xiong et al. 2019a). As shown in Fig. 6, the typical regions and major cities are Bangkok, Kuala Lumpur, Bangalore, Cairo, Riyadh, Moscow, and Kyiv. Here, the response to floods mainly depends on the various flood defense structures. However, there will be many difficulties in mitigating flood vulnerability if people only rely on flood defense structures. Methods, such as "living with rivers" and "making space for water," not only provide space for storing flood water, but also protect natural habitats (Johnson et al. 2007).

5.3 Importance and limitations

The United Nations Disaster Reduction Agency (UNISDR, 2011) recently stated that the exposure of economies affected by floods is increasing in all regions of the world, while the risk of death in developed countries is declining due to the increased income and improved

governance (i.e., the emergency planning and preparations) (Jongman et al. 2012). How-ever, most of the countries in the Belt and Road region are developing countries with lim-ited levels of economic, social, technological and educational development, leading to their disaster prevention capabilities and mitigation foundations and abilities are weak relatively (Ge et al. 2020). In addition, these countries are focusing more on building their econo-mies, while ignoring the constructions of disaster prevention and mitigation systems (Gray and Mueller 2012; Jongman et al. 2012; Tanoue et al. 2016). In the cities and regions that are more susceptible to disasters, regardless of whether the risks are to human lives or the economies, the preventions and mitigations of floods should be emphasized. Subsequently, flood awareness should be increased to deal with flood risks in a sustainable way (Johnson et al. 2007). Currently, more reliable vulnerability studies need to be conducted for the entire Belt and Road region, and this study contributes to this need.

Despite progress being made via this study, there are limitations to this study. Initially, a larger resolution was considered for use (i.e., 1×1 km or 0.5×0.5 km) (Ding et al. 2016), but later it was found that there were millions of grids corresponding to these resolutions, which was a huge test for the experimental equipment used. Regrettably, we only con-ducted the spatial analysis of the vulnerability, not the temporal analysis. In this study, due to the large area of the Belt and Road region and the availability of data, some common indicators were not included (i.e., the literacy rate, cultural level, existing medical condi-tions, and unemployment rates) (Ding et al. 2016; Hoque et al. 2019; Lee et al. 2015). Additionally, the GDP per capita data used were calculated by GDP and population data and may decrease the accuracy of the results. In fact, there is still a lack of a consistent set of metrics to measure flood vulnerability, because the understandings of vulnerability are different among scholars (Janssen et al. 2006; Liverman and O'Brien 1991). However, the index system is a vital step in flood vulnerability assessment (Ding et al. 2016; Lyu et al. 2020b); thus, future studies should consider the influences of these factors, and this aspect should prove to be an interesting topic.

6 Conclusions

We proposed a quantitative model of indexes based on the TFN-AHP and the SVM model. A map of the Belt and Road region of flood vulnerability profile was generated. Firstly, we prepared a database including 11 flood influential factors that were classified into five levels. Then, the exposure and disaster reduction capability were quantified based on the TFN-AHP and SVM model, respectively. Finally, the spatial distribution of the exposure, the disaster reduction capability, and the vulnerability in the Belt and Road region were generated and analyzed. Although this study has limitations in terms of the temporal scale and spatial resolution, the results for the high-vulnerability regions will hopefully encour-age local government officials to pay attention to "hot spots" where more accurate analyses need to be conducted. Through the analysis of exposure, disaster reduction capability and vulnerability results, the following conclusions can be drawn: (1) The high-exposure areas are primarily distributed in areas with higher population densities, more built-up land, and relatively developed economies. (2) The disaster reduction capabilities of the coun-tries along the Belt and Road are inextricably linked to their socioeconomic development. The areas with high disaster reduction capability are mainly concentrated in the major cities in the Belt and Road region (i.e., Beijing, Shanghai, Hong Kong, Taipei, Bangkok, Jakarta, New Delhi, Riyadh, Abu Dhabi, Cairo). (3) The vulnerability patterns are largely

determined by exposure, while the disaster reduction capability may alleviate flood pressure at local scales. The high-vulnerable areas (accounting for 3.54%) are primarily distributed in southern and eastern China, northern India, most of Bangladesh, the Indus Valley in Pakistan, the Nile River Basin in Egypt, the central region of Indonesia, and the major cities in the Belt and Road region. Obviously, these highly vulnerable regions and cities coincide with the areas that are characterized by frequent economic activities and dense populations, indicating that areas with high populations and economic densities may be more susceptible to flood disasters in the future.

Data availability The population data are available at https://www.worldpop.org/ (last access: April 2019). The land use data are available at https://ladsweb.modaps.eosdis.nasa.gov/ (last access: September 2019). The GDP data are available at https://datadryad.org/stash/dataset/doi:10.5061/dryad.dk1j0 (last access: October 2019). The data connected with infrastructure, including data from hospitals, shelters, and road density data, are available at https://www.openstreetmap.org/ (last access: December 2019). The digital elevation model (DEM) data are available at http://srtm.csi.cgiar.org/srtmdata/ (last access: September 2018). The impervious surface data are available at https://ghslsys.jrc.ec.europa.eu/ (last access: December 2019).

Declarations

References

Adger WN (2006) Vulnerability. Glob Environ Change 16(3):268–281. https://doi.org/10.1016/j.gloenvcha.2006.02.006

Adikari Y, Osti R, Noro T (2010) Flood-related disaster vulnerability: an impending crisis of megacities in Asia. J Flood Risk Manag 3(3):185–191. https://doi.org/10.1111/j.1753-318X.2010.01068.x

An Y, Tan X-C, Gu B-H, Zhu K-W (2020) Flood risk assessment using the CV-TOPSIS method for the Belt and Road Initiative: an empirical study of Southeast Asia. Ecosys Health Sustain. https://doi.org/10.1080/20964129.2020.1765703

Atangana Njock PG, Shen S-L, Zhou A-N, Lyu H-M (2020) Evaluation of soil liquefaction using AI technology incorporating a coupled ENN/t-SNE model. Soil Dyn Earthq Eng 130:105988. https://doi.org/10.1016/j.soildyn.2019.105988

Bodoque JM, Amerigo M, Díez-Herrero A et al (2016) Improvement of resilience of urban areas by integrating social perception in flash-flood risk management. J Hydrol 541:665–676. https://doi.org/10.1016/j.jhydrol.2016.02.005

Bouwer LM, Bubeck P, Aerts JCJH (2010) Changes in future flood risk due to climate and development in a Dutch polder area. Glob Environ Change 20(3):463–471. https://doi.org/10.1016/j.gloenvcha.2010.04.002

Bui DT, Pradhan B, Lofman O, Revhaug I (2012) Landslide susceptibility assessment in vietnam using support vector machines, decision tree, and naive bayes models. Math Probl Eng 2012:26. https://doi.org/10.1155/2012/974638

Cascini L (2008) Applicability of landslide susceptibility and hazard zoning at different scales. Eng Geol 102(3–4):164–177. https://doi.org/10.1016/j.enggeo.2008.03.016

Chen H-L, Ito Y, Sawamukai M, Tokunaga T (2015) Flood hazard assessment in the Kujukuri Plain of Chiba Prefecture, Japan, based on GIS and multicriteria decision analysis. Nat Hazards 78(1):105–120. https://doi.org/10.1007/s11069-015-1699-5

Cheng Z-L, Zhou W-H, Garg A (2020) Genetic programming model for estimating soil suction in shallow soil layers in the vicinity of a tree. Eng Geol 268:105506. https://doi.org/10.1016/j.enggeo.2020.105506

Cherkassky V (1997) The nature of statistical learning theory. IEEE Trans Neural Netw 8(6):1564–1564. https://doi.org/10.1109/TNN.1997.641482

Cui P, Wu S-N, Lei Y, Zhang Z-T, Zou Q (2020) Disaster risk management pattern along the Belt and Road regions. Sci Technol Rev 38(16):35–44. https://doi.org/10.3981/j.issn.1000-7857.2020.16.004

Cutter SL (2003) Social vulnerability to environmental hazards. Soc Sci Q. https://doi.org/10.1111/1540-6237.8402002

Cutter SL, Finch C (2008) Temporal and spatial changes in social vulnerability to natural hazards. Proc Natl Acad Sci USA 105(7):2301–2306. https://doi.org/10.1073/pnas.0710375105

de Moel H, Aerts JCJH (2011) Effect of uncertainty in land use, damage models and inundation depth on flood damage estimates. Nat Hazards 58(1):407–425. https://doi.org/10.1007/s11069-010-9675-6

Ding M-T, Heiser M, Hubl J, Fuchs S (2016) Regional vulnerability assessment for debris flows in China—a CWS approach. Landslides 13(3):537–550. https://doi.org/10.1007/s10346-015-0578-1

Erena SH, Worku H (2019) Urban flood vulnerability assessments: the case of Dire Dawa city. Ethiop Nat Hazards 97(2):495–516. https://doi.org/10.1007/s11069-019-03654-9

Eric N, Thomas P (2007) The gendered nature of natural disasters: the impact of catastrophic events on the gender gap in life expectancy, 1981–2002. Ann Am as Geogr 97(3):551–566. https://doi.org/10.1111/j.1467-8306.2007.00563.x

Fang J, Li M-J, Wang J-A, Shi P-J (2015) Assessment and mapping of global fluvial flood risk. J Nat Disasters 24(01):1–8. https://doi.org/10.13577/j.jnd.2015.0101

Fang Y, Yin J, Wu B-H (2016) Flooding risk assessment of coastal tourist attractions affected by sea level rise and storm surge: a case study in Zhejiang Province. China Nat Hazards 84(1):611–624. https://doi.org/10.1007/s11069-016-2444-4

Fekete A (2012) Spatial disaster vulnerability and risk assessments: challenges in their quality and acceptance. Nat Hazards 61(3):1161–1178. https://doi.org/10.1007/s11069-011-9973-7

Franklin J (2005) The elements of statistical learning: data mining, inference and prediction. Math Intell 27(2):83–85. https://doi.org/10.1007/BF02985802

Fraser EDG, Dougill AJ, Mabee WE, Reed M, Mcalpine P (2006) Bottom up and top down: analysis of participatory processes for sustainability indicator identification as a pathway to community empowerment and sustainable environmental management. J Environ Manag 78(2):114–127. https://doi.org/10.1016/j.jenvman.2005.04.009

Gallopín G (2006) Linkages between vulnerability, resilience, and adaptive capacity. Glob Environ Change 16(3):293–303. https://doi.org/10.1016/j.gloenvcha.2006.02.004

Ge Y-G, Cui P, Chen X-Q (2020) Strategy of the international cooperation with respect to disaster prevention and reduction in the Belt and Road areas. Sci Technol Rev 38(16):29–34. https://doi.org/10.3981/j.issn.1000-7857.2020.16.003

Gray C, Mueller V (2012) Drought and population mobility in rural ethiopia. World Dev 40(1):134–145. https://doi.org/10.1016/j.worlddev.2011.05.023

Hafeez M, Yuan C-H, Shahzad K, Aziz B, Iqbal K, Raza S (2019) An empirical evaluation of financial development-carbon footprint nexus in One Belt and Road region. Environ Sci Pollut Res 26(24):25026–25036. https://doi.org/10.1007/s11356-019-05757-z

He Y-Y, Zhou J-Z, Kou P-G, Lu N, Zou Q (2011) A fuzzy clustering iterative model using chaotic differential evolution algorithm for evaluating flood disaster. Expert Syst Appl 38(8):10060–10065. https://doi.org/10.1016/j.eswa.2011.02.003

Hoque MA, Tasfia S, Ahmed N, Pradhan B (2019) Assessing spatial flood vulnerability at Kalapara Upazila in Bangladesh using an analytic hierarchy process. Sensors 19(6):1302. https://doi.org/10.3390/s19061302

Hu P, Zhang Q, Shi P-J, Chen B, Fang J-Y (2018) Flood-induced mortality across the globe: spatiotemporal pattern and influencing factors. Sci Total Environ 643:171–182. https://doi.org/10.1016/j.scitotenv.2018.06.197

Huang J-Y, Liu Y, Ma L (2011) Assessment of regional vulnerability to natural hazards in China using a DEA model. Int J Disaster Risk Sci 2(2):41–48. https://doi.org/10.1007/s13753-011-0010-y

Janssen MA, Schoon ML, Ke W, Börner K (2006) Scholarly networks on resilience, vulnerability and adaptation within the human dimensions of global environmental change. Glob Environ Change 16(3):240–252. https://doi.org/10.1016/j.gloenvcha.2006.04.001

Johnson C, Penning-Rowsell E, Tapsell S (2007) Aspiration and reality: flood policy, economic damages and the appraisal process. Area 39(2):214–223. https://doi.org/10.1111/j.1475-4762.2007.00727.x

Jongman B, Ward PJ, Aerts JCJH (2012) Global exposure to river and coastal flooding: long term trends and changes. Glob Environ Change 22(4):823–835. https://doi.org/10.1016/j.gloenvcha.2012.07.004

Jongman B, Winsemius HC, Aerts JCJH et al (2015) Declining vulnerability to river floods and the global benefits of adaptation. Proc Natl Acad Sci USA 112(18):E2271–E2280. https://doi.org/10.1073/pnas.1414439112

Kim ES, Choi HI (2011) Assessment of vulnerability to extreme flash floods in design storms. Int J Environ Res Public Health 8(7):2907–2922. https://doi.org/10.3390/ijerph8072907

Komolafe AA, Herath S, Avtar R (2019) Establishment of detailed loss functions for the urban flood risk assessment in Chao Phraya River basin, Thailand. Geom Nat Hazards Risk 10(1):633–650. https://doi.org/10.1080/19475705.2018.1539038

Kummu M, Taka M, Guillaume JHA (2018) Data descriptor: gridded global datasets for gross domestic product and human development index over 1990–2015. Sci Data 5:15. https://doi.org/10.1038/sdata.2018.4

Lee S, Okazumi T, Kwak Y, Takeuchi K (2015) Vulnerability proxy selection and risk calculation formula for global flood risk assessment: a preliminary study. Water Policy 17(1):8. https://doi.org/10.2166/wp.2014.158

Li Z-H, Nadim F, Huang H-W, Uzielli M, Lacasse S (2010) Quantitative vulnerability estimation for scenario-based landslide hazards. Landslides 7(2):125–134. https://doi.org/10.1007/s10346-009-0190-3

Li L-T, Xu Z-X, Pang B, Liu L (2012) Flood risk zoning in China. J Hydraul Eng 43(1):22–30. https://doi.org/10.13243/j.cnki.slxb.2012.01.001

Liu X-L, Lei J-Z (2003) A method for assessing regional debris flow risk: an application in Zhaotong of Yunnan province (SW China). Geomorphology. https://doi.org/10.1016/S0169-555X(02)00242-8

Liu J, Wang S-Y (2013) Analysis of human vulnerability to the extreme rainfall event on 21–22 July 2012 in Beijing. China Natural Hazards Earth Sys Sci 13(11):2911–2926. https://doi.org/10.5194/nhess-13-2911-2013

Liu J-F, Wang X-Q, Zhang B, Li J, Zhang J-Q, Liu X-Q (2017a) Storm flood risk zoning in the typical regions of Asia using GIS technology. Nat Hazards 87(3):1691–1707. https://doi.org/10.1007/s11069-017-2843-1

Liu X-L, Cheng M, Tian C-S (2017b) Comparative analysis of two methods for assessing hazard of landslide and debris-flow on a regional scale. J Disaster Prev Mitig Eng. https://doi.org/10.13409/j.cnki.jdpme.2017.01.010

Liu Y-S, Yang Z-S, Huang Y-H, Liu C-J (2018) Spatiotemporal evolution and driving factors of China's flash flood disasters since 1949. Sci China-Earth Sci 61(12):1804–1817. https://doi.org/10.1007/s11430-017-9238-7

Liu Y-X, Zhao W-W, Hua T, Wang S, Fu B-J (2019) Slower vegetation greening faced faster social development on the landscape of the Belt and Road region. Sci Total Environ. https://doi.org/10.1016/j.scitotenv.2019.134103

Liverman D, O'Brien K (1991) Global warming and climate change in Mexico. Glob Environ Change 1(5):351–364. https://doi.org/10.1016/0959-3780(91)90002-B

Lugeri N, Kundzewicz ZW, Genovese E, Hochrainer S, Radziejewski M (2010) River flood risk and adaptation in Europe—assessment of the present status. Mitig Adapt Strat Glob Change 15(7):621–639. https://doi.org/10.1007/s11027-009-9211-8

Lyu H-M, Shen S-L, Yang J, Yin Z-Y (2019a) Inundation analysis of metro systems with the storm water management model incorporated into a geographical information system: a case study in Shanghai. Hydrol Earth Syst Sci 23(10):4293–4307. https://doi.org/10.5194/hess-23-4293-2019

Lyu H-M, Shen S-L, Zhou A-N, Zhou W-H (2019b) Flood risk assessment of metro systems in a subsiding environment using the interval FAHP-FCA approach. Sustain Cities Soc 50:101682. https://doi.org/10.1016/j.scs.2019.101682

Lyu H-M, Shen S-L, Zhou A-N, Yang J (2020a) Risk assessment of mega-city infrastructures related to land subsidence using improved trapezoidal FAHP. Sci Total Environ 717:135310. https://doi.org/10.1016/j.scitotenv.2019.135310

Lyu H-M, Zhou W-H, Shen S-L, Zhou A-N (2020b) Inundation risk assessment of metro system using AHP and TFN-AHP in Shenzhen. Sustain Cities 56:102103. https://doi.org/10.1016/j.scs.2020.102103

Mahmoud SH, Gan TY (2018) Multi-criteria approach to develop flood susceptibility maps in arid regions of Middle East. J Clean Prod 196:216–229. https://doi.org/10.1016/j.jclepro.2018.06.047

Malone EL, Engle NL (2011) Evaluating regional vulnerability to climate change: purposes and methods. Wiley Interdiscip Rev Clim Change 2(3):462–474. https://doi.org/10.1002/wcc.116

Metzger MJ, Rounsevell MDA, Acosta-Michlik L, Leemans R, Schröter D (2006) The vulnerability of ecosystem services to land use change. Agr Ecosyst Environ 114(1):69–85. https://doi.org/10.1016/j.agee.2005.11.025

Ntajal J, Lamptey BL, Mahamadou IB, Nyarko BK (2017) Flood disaster risk mapping in the Lower Mono River Basin in Togo, West Africa. Int J Disaster Risk Reduct 23:93–103. https://doi.org/10.1016/j.ijdrr.2017.03.015

Okazawa Y, Yeh PJF, Kanae S, Oki T (2011) Development of a global flood risk index based on natural and socio-economic factors. Hydrol Sci J 56(5):789–804. https://doi.org/10.1080/02626667.2011.583249

Rana IA, Routray JK (2018) Integrated methodology for flood risk assessment and application in urban communities of Pakistan. Nat Hazards 91(1):239–266. https://doi.org/10.1007/s11069-017-3124-8

Rani NNVS, Satyanarayana ANV, Bhaskaran PK (2015) Coastal vulnerability assessment studies over India: a review. Nat Hazards 77(1):405–428. https://doi.org/10.1007/s11069-015-1597-x

Rawat PK, Pant CC, Tiwari PC, Sharma PDPK (2012) Spatial variability assessment of river-line floods and flash floods in Himalaya. Disaster Prev Manag 21(2):135–159. https://doi.org/10.1108/09653561211219955

Rimba AB, Setiawati MD, Sambah AB, Miura F (2017) Physical flood vulnerability mapping applying geospatial techniques in Okazaki City, Aichi Prefecture. Jpn Urban Sci 1(7):1–22. https://doi.org/10.3390/urbansci1010007

Sam AS, Kumar R, Kachele H, Muller K (2017) Vulnerabilities to flood hazards among rural households in India. Nat Hazards 88(2):1133–1153. https://doi.org/10.1007/s11069-017-2911-6

Sampson CC, Fewtrell TJ, Duncan A, Shaad K, Horritt MS, Bates PD (2012) Use of terrestrial laser scanning data to drive decimetric resolution urban inundation models. Adv Water Resour 41:1–17. https://doi.org/10.1016/j.advwatres.2012.02.010

Sharma SVS, Roy PS, Chakravarthi V, Rao GS (2018) Flood risk assessment using multi-criteria analysis: a case study from Kopili River Basin, Assam, India. Geom Nat Hazards Risk 9(1):79–93. https://doi.org/10.1080/19475705.2017.1408705

Shi Y (2013) Population vulnerability assessment based on scenario simulation of rainstorm-induced waterlogging: a case study of Xuhui District, Shanghai city. Nat Hazards 66(2):1189–1203. https://doi.org/10.1007/s11069-012-0544-3

Shi Y, Xu S-Y, Shi C (2011) Progress in research on vulnerability of natural disasters. J Natl Disasters 20(02):131–137. https://doi.org/10.13577/j.jnd.2011.0221

Spitalar M, Gourley JJ, Lutoff C, Kirstetter PE, Brilly M, Carr N (2014) Analysis of flash flood parameters and human impacts in the US from 2006 to 2012. J Hydrol 519:863–870. https://doi.org/10.1016/j.jhydrol.2014.07.004

Tanoue M, Hirabayashi Y, Ikeuchi H (2016) Global-scale river flood vulnerability in the last 50 years. Sci Rep 6:9. https://doi.org/10.1038/srep36021

Tehrany MS, Pradhan B, Jebur MN (2013) Spatial prediction of flood susceptible areas using rule based decision tree (DT) and a novel ensemble bivariate and multivariate statistical models in GIS. J Hydrol 504:69–79. https://doi.org/10.1016/j.jhydrol.2013.09.034

Tehrany MS, Pradhan B, Jebur MN (2014) Flood susceptibility mapping using a novel ensemble weights-of-evidence and support vector machine models in GIS. J Hydrol 512(6):332–343. https://doi.org/10.1016/j.jhydrol.2014.03.008

Tehrany MS, Pradhan B, Mansor S, Ahmad N (2015) Flood susceptibility assessment using GIS-based support vector machine model with different kernel types. CATENA 125:91–101. https://doi.org/10.1016/j.catena.2014.10.017

Wan SA, Lei TC (2009) A knowledge-based decision support system to analyze the debris-flow problems at Chen-Yu-Lan River, Taiwan. Knowl Based Syst 22(8):580–588. https://doi.org/10.1016/j.knosys.2009.07.008

Weis SWM, Agostini VN, Roth LM et al (2016) Assessing vulnerability: an integrated approach for mapping adaptive capacity, sensitivity, and exposure. Clim Change 136(3):615–629. https://doi.org/10.1007/s10584-016-1642-0

Werren G, Reynard E, Lane SN, Balin D (2016) Flood hazard assessment and mapping in semi-arid pied-mont areas: a case study in Beni Mellal, Morocco. Nat Hazards 81(1):481–511. https://doi.org/10.1007/s11069-015-2092-0

Wu J, Yang R, Song J (2018) Effectiveness of low-impact development for urban inundation risk mitigation under different scenarios: a case study in Shenzhen, China. Nat Hazards Earth Syst Sci 18(9):2525–2536. https://doi.org/10.5194/nhess-18-2525-2018

Xia F-Q, Kang X-W, Wu S-H et al (2008) Research on dike breach risk of the hanging reach under different flood conditions in the Lower Yellow River. Geogr Res 27(1):229–239

Xian S-D (2010) A new fuzzy comprehensive evaluation model based on the support vector machine. Fuzzy Inf Eng 2(1):75–86. https://doi.org/10.1007/s12543-010-0038-5

Xiong J-N, Li J, Cheng W-M, Wang N, Guo L (2019a) A GIS-based support vector machine model for flash flood vulnerability assessment and mapping in China. Int J Geo-Inf 8(7):297. https://doi.org/10.3390/ijgi8070297

Xiong J-N, Sun M, Zhang H et al (2019b) Application of the Levenburg-Marquardt back propagation neural network approach for landslide risk assessments. Nat Hazards Earth Syst Sci 19(3):629–653. https://doi.org/10.5194/nhess-19-629-2019

Xu C, Dai F-C, Xu X-W, Lee YH (2012) GIS-based support vector machine modeling of earthquake-triggered landslide susceptibility in the Jianjiang River watershed, China. Geomorphology 145–146:70–80. https://doi.org/10.1016/j.geomorph.2011.12.040

Yang X-L, Ding J-H, Hou H (2013) Application of a triangular fuzzy AHP approach for flood risk evaluation and response measures analysis. Nat Hazards 68(2):657–674. https://doi.org/10.1007/s11069-013-0642-x

Yao X, Tham LG, Dai F-C (2008) Landslide susceptibility mapping based on support vector machine: a case study on natural slopes of Hong Kong, China. Geomorphology 101(4):572–582. https://doi.org/10.1016/j.geomorph.2008.02.011

Zhang Z-G (2014) Research on rainstorm waterlogging risk assessment of urban comminities—a case of Jinsha community. Shanghai Normal University, Shanghai

Zhang Y-L, You W-J (2014) Social vulnerability to floods: a case study of Huaihe River Basin. Nat Hazards 71(3):2113–2125. https://doi.org/10.1007/s11069-013-0996-0

Zhou Y, Li N, Wu W-X, Wu J-D (2014) Assessment of provincial social vulnerability to natural disasters in China. Nat Hazards 71(3):2165–2186. https://doi.org/10.1007/s11069-013-1003-5

Zhou S-E, Zhang M-J, Wang S-J (2018) Assessment of vulnerability in natural-social system in Hexi, Gansu. Resour Sci 40(2):452–462. https://doi.org/10.18402/resci.2018.02.20

Zhou J, Jiang T, Wang Y-J, Su B-D, Zhai J-Q (2020) Spatiotemporal variations of aridity index over the Belt and Road region under the 1.5°C and 2.0°C warming scenarios. J Geograph Sci 30(1):37–52. https://doi.org/10.1007/s11442-020-1713-z

Zong N (2013) Flood hazard vulnerability and risk assessment of urban community—a case study of Shanghai. East China Normal University.

Authors and Affiliations

Yu Duan[1] · Junnan Xiong[1,2] · Weiming Cheng[2,3] · Nan Wang[2,3] · Yi Li[4] · Yufeng He[1] · Jun Liu[1] · Wen He[1] · Gang Yang[1]

Yu Duan
201922000658@stu.swpu.edu.cn

Weiming Cheng
chengwm@lreis.ac.cn

Nan Wang
wangnd.17b@igsnrr.ac.cn

Yi Li
liyi@aircas.ac.cn

Yufeng He
201922000656@stu.swpu.edu.cn

Jun Liu
201922000655@stu.swpu.edu.cn

Wen He
201922000663@stu.swpu.edu.cn

Gang Yang
201922000664@stu.swpu.edu.cn

[1]   School of Civil Engineering and Geomatics, Southwest Petroleum University, Chengdu 640500, China

[2]   State Key Laboratory of Resources and Environmental Information System, Institute of Geographic Sciences and Natural Resources Research, CAS, Beijing 100101, China

[3]   University of Chinese Academy of Sciences, Beijing 100049, China

[4]   Aerospace Information Research Institute, CAS, Beijing 100094, China